Influence of winding layout and airgap length on radial forces in large synchronous hydrogenerators

Erlend L. Engevik, Mostafa Valavi, and Arne Nysveen

Department of Electric Power Engineering, Norwegian University of Science and Technology (NTNU), Trondheim, Norway

Email: erlend.engevik@ntnu.no

Abstract—This paper investigates the flux density and radial force spatial harmonics in large salient pole synchronous hydrogenerators. Vibration due to magnetic forces are mainly caused by low order harmonics in the airgap flux density distribution. The influence of winding layout and airgap length on the lowest order radial force component are analysed. Airgap flux density and radial force density distributions of three different generators are computed using finite element calculations. The flux density components that contributes to the lowest order force component, and the source for these harmonic components, are investigated. It is found that reducing the airgap length leads to a less than proportional increase in the lowest order radial force component. A rearrangement of the winding layout is found to be an effective method for reducing the lowest order radial force component.

Index Terms—Fractional-slot windings, hydrogenerators, radial forces, vibration

I. INTRODUCTION

Most hydrogenerators are salient pole synchronous generators with relatively low speed of rotation and a high number of poles. Several advantages of fractional-slot windings over integer-slot windings are given in [1]. It gives greater freedom of choice when selecting the number of slots, several alternatives for short pitching and it is easier to achieve lower harmonic distortion (i.e. reduced 3rd, 5th, 7th and higher order harmonics) [2].

Fractional-slot windings produce subharmonic field waves, which are field waves with wavelengths larger than the wavelength of the main harmonic. These subharmonics can cause unwanted parasitic effects [2].

Variable speed operation of hydropower plants using the converter-fed synchronous machine (CFSM) topology makes it possible to rethink the design requirements that grid-connected generators face today. The CFSM topology is especially suited for pumped storage plants and power plants with large variations in water flow or hydraulic head throughout the year [3].

In [4] it is concluded that lifting the requirement on the synchronous reactance can reduce the cost of the generator by reducing the airgap length. One question that comes up if the airgap length is reduced is will this lead to unacceptable increases in the radial forces that can cause vibration problems?

When designing large hydrogenerators with fractional-slot windings, the chosen combination of stator slots and poles

will determine the lowest mode of vibration [5]. If the initial slot/pole-combination results in radial forces with a very low harmonic order, the number of slots can be changed to increase the order of the lowest radial force harmonic. If the lowest harmonic order of the radial forces is increased, the risk for having vibration problems is reduced.

In existing, large hydrogenerators with fractional-slot windings there are several methods to reduce vibration problems. The winding can be made into an integer-slot configuration, the pole and slot configuration can be changed, the eigenfrequency of the stator construction can be changed, or the existing winding configuration can be changed. The last option is usually the best and least expensive option if the generator is already built.

It is possible to introduce variable-speed operation by upgrading existing generators. This can be done by equipping the generator with a full-rated frequency converter. Another option is to retrofit the machine into a doubly-fed induction generator (DFIG) by replacing the salient pole rotor with a new, round rotor. This was done for a 12 MVA, 102-slot/10-pole generator in [6]. The airgap length was reduced from 20 mm to 6 mm, resulting in a severe vibration problem.

The solution that was chosen to reduce the vibration was to rearrange the winding configuration [7]. Similarly, in [8], an existing 360 MVA, 168-slot/20-pole generator was experiencing low order vibration problems. By changing the winding pattern, it was possible to reduce the radial force component that caused vibrations considerably.

It was claimed in [6] that the reduction in airgap gave a proportional increase in the main flux density component that interacted to produce most of the lowest order radial force component. Similar studies, where the airgap length is reduced, has not been found for large, salient pole synchronous hydrogenerators. In this paper, the influence of a reduced airgap length on the lowest order radial force component will be investigated.

Three generators are analysed with the design specifications given in Table I. It was chosen to have both low-speed and high-speed generators, and machines with both a high and a lower number of slots per pole and phase. All simulations are made using stationary finite element simulations. No time-dependent effects, like the impact of having damper bars, are taken into account in this study.

TABLE I:
Design specifications

	G1	G2	G3
Power (MVA)	105	320	105
Speed (rpm)	428.6	428.6	85.7
Number of poles	14	14	70
Number of slots	180	114	432
Airgap diameter (m)	3.672	4.364	12.0
Machine length (m)	1.8	3.6	0.96

II. ANALYSIS OF FLUX DENSITY HARMONICS

In order to study the causes of the radial forces in the generators based on the Maxwell stress tensor, the spatial harmonic orders of the radial flux density are investigated.

The radial spatial harmonic flux density distribution for all three generators at both no-load and full-load are presented in Fig. 1. The main flux density harmonic is equal to the pole pair number p. Spatial harmonic orders of odd multiples of the pole pair number are present at no-load.

In addition, spatial harmonics due to slotting are also present. Some of these harmonics, like the ones of order $Q_s \pm p$, have a considerable amplitude. Q_s is the number of slots in the stator. For the 114-slot/14-pole generator, harmonic orders 107 and 121 are produced by the slotting effect, while for the 180-slot/14-pole generator harmonic orders 173 and 187 are present due to slotting. In the case of the 432-slot/70-pole generator, the 397th and 467th harmonics are produced by slotting.

One can see from Fig. 1 that several harmonic orders that are not present at no-load are visible in the full-load case. Subharmonics, harmonics adjacent to the main harmonic, and harmonics adjacent to the harmonic of order $3p$ are produced by the armature mmf.

As can be seen in Fig. 2, a small subharmonic of order 1 can be seen in all three generators. The order of the lowest-order spatial flux density harmonic is equal to the greatest common divisor (GCD) of Q_s and p. The GCD of Q_s and p is 1 for all three generators studied in this paper. All generators were selected to have the lowest possible order of the radial force component.

Several analytical methods have been used for predicting and analysing the harmonic content in the airgap of large hydrogenerators. Often the mmf harmonics are calculated analytically based on the winding layout [8]. The airgap flux density harmonics are then calculated using airgap permeance formulations, where influence of the permeance of the rest of the generator is assumed negligible [2],[7].

It is also possible to use the winding factor of the different mmf harmonics [9] to predict the amplitude of the flux density harmonics. These are all simplified methods, and one cannot be sure that the amplitudes of the different flux density harmonics are calculated correctly. In order to do this, finite element simulations are needed. The amplitude of the flux density harmonics need to be calculated correctly if the
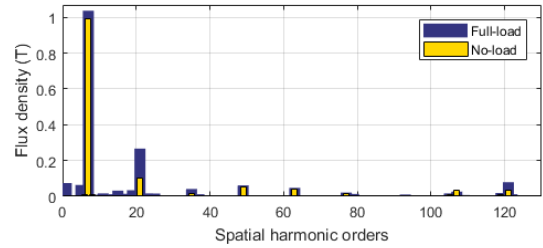

(a) 114-slot, 14-pole generator
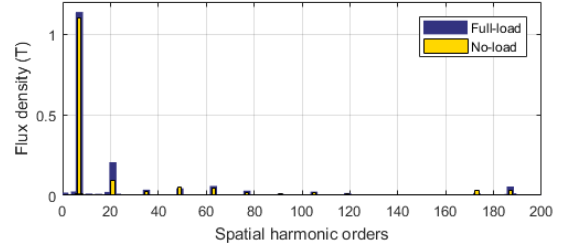
(b) 180-slot, 14-pole generator
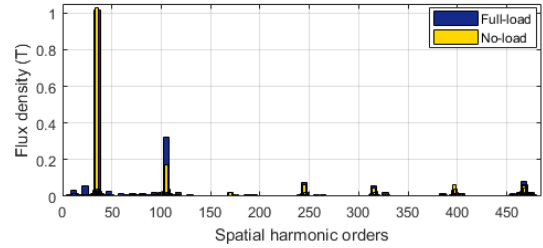
(c) 432-slot, 70-pole generator

Fig. 1: Harmonic orders of flux density in the airgap at full-load and no-load.

amplitude of the lowest order radial force component is to be calculated.
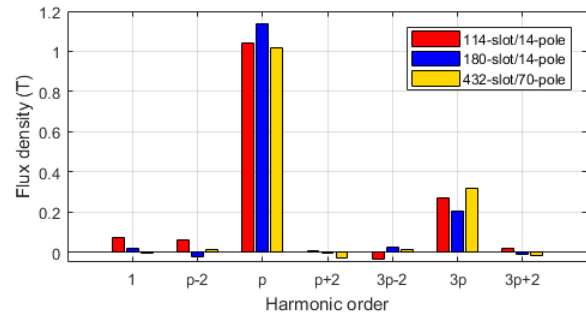
Fig. 2: Spatial harmonic orders of flux density contributing to the production of 2nd order radial force harmonic.

III. ANALYSIS OF RADIAL FORCE DENSITY

Radial magnetic forces are among the main sources for vibration in the generator. In order to calculate the radial force
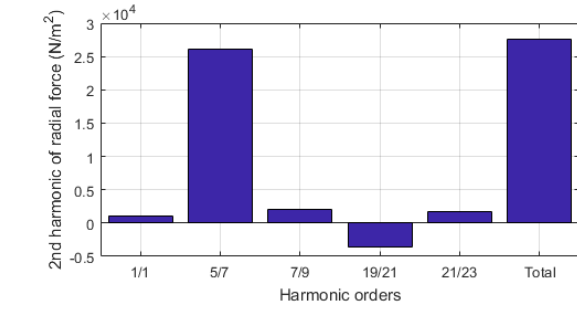
(a) 114-slot, 14-pole generator
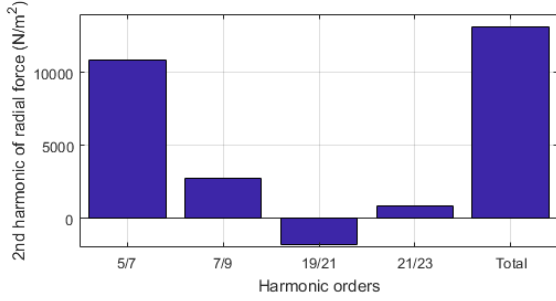
(b) 180-slot, 14-pole generator
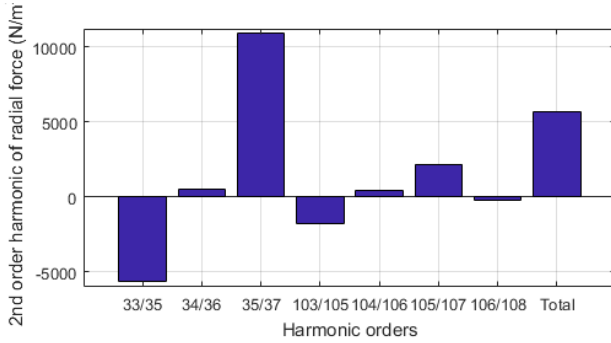

(c) 432-slot, 70-pole generator

Fig. 3: Contribution of different flux density harmonics that produce the 2nd harmonic order on radial force distribution

density, the Maxwell stress tensor is employed to calculate the radial force density f_r with (1).

$$f_r = \frac{1}{2\mu_0}\left(B_r^2 - B_t^2\right) \tag{1}$$

When considering potential electromagnetic causes for vibration in rotating electrical machine, it is mostly radial forces with low harmonic orders that can be problematic. The amplitude of deformation is inversely proportional to m^4 [10], where m is the harmonic order. Vibration in the machine is mainly given by the lowest mode of vibration [5]. The lowest mode of vibration is equal to the GCD of Q_s and $2p$, which is two in the generators considered in this paper [5].

Low-speed generators are more susceptible to having vibration problems than high-speed generators at the same amplitude of the lowest order radial force component [10]. The amplitude of deformation is increased when the diameter of

the generator is increased, and when the thickness of the stator yoke is reduced. Both are the case for low-speed generators since they have a high number of poles.

The radial component of the force density f_r as expressed by (1) can be written as the contributions of the radial components of the flux density f_{rr} minus the contributions from the tangential flux density components f_{rt}, (2).

$$f_r = f_{rr} - f_{rt} = \left(\frac{1}{2\mu_0}B_r^2\right) - \left(\frac{1}{2\mu_0}B_t^2\right) \tag{2}$$

It is investigated how different harmonic pairs in flux density whose harmonic order differs by two (order i and j that gives $i - j = 2$) contribute to the produce the 2nd order radial force harmonic. In the generators considered, the tangential flux density harmonics were found to contribute with less than 1 % of the 2nd order radial force density. It is therefore neglected in the further analysis.

The 2nd order harmonic radial force component that is caused by the radial flux density components f_{rr} can be expressed as (3).

$$f_{rr}(2^{nd}) = \frac{1}{2\mu_0}\left[\frac{1}{2}B_{r1}^2 + \sum_{k=1,2,3}^{\infty}B_{rk}\cdot B_{r(k+2)}\right]cos(2\theta) \tag{3}$$

where k is the spatial harmonic order and B_{rk} is the airgap flux density component of harmonic order k. From Fig 2, it can be seen that only a few harmonic components of the airgap flux density of the 14-pole generators have amplitudes large enough to be included in equation (3). Based on this, the 2nd spatial harmonic component of f_{rr} of the 114-slot/14-pole generator can be written as (4).

$$f_{rr}(2^{nd}) = \frac{1}{2\mu_0}(\frac{1}{2}B_1B_1 + B_5B_7 + B_7B_9 + B_{19}B_{21} + B_{21}B_{23}) \tag{4}$$

It is observed that the amplitude and sign of the flux density harmonics in (4) determines the amplitude of the 2nd order harmonic force component. From Fig. 2 it is seen that the 1st, 5th, 7th, 9th, 21st and 23rd of the 114-slot/14-pole generator have the same sign. The 19th harmonic have the opposite sign.

In Fig. 3a we have that the interaction between the flux density harmonics of orders 5/7, 7/9 and 21/23 contribute to increasing the total 2nd order radial force density. In the 114-slot/14-pole generator the square of the first order harmonic (4) gives a small contribution to the increase in the 2nd order radial force component. The interaction between the harmonic pair of orders 19/21 contributes to a reduction in the total 2nd order radial force density.

The same analysis applies to the 180-slot/14-pole generator, see Fig. 3b. It is the same pairs of flux density harmonics that contribute to the 2nd order force component. In the 180-slot/14-pole generator and the 432-slot/70-pole generator, the amplitude of the first order flux density harmonic is so small that the contribution to the 2nd order force component is negligible.

For the 70-pole generator, it is also seen in Fig. 2 that there are only a few harmonic components that contribute to the 2nd order component of f_{rr}. Similar to the 14-pole generators, the 2nd harmonic component of f_{rr} can be written as (5).

$$f_{rr}(2^{nd}) = \frac{1}{2\mu_0}(B_{33}B_{35} + B_{34}B_{36} + B_{35}B_{37} + B_{103}B_{105} + B_{104}B_{106} + B_{105}B_{107} + B_{106}B_{108}) \tag{5}$$

From Fig. 2 it is seen that the 33rd, 35th, 103rd and 105th flux density harmonic of the 432-slot/70-pole generator have the same sign. The 37th and the 107th flux density harmonic have the opposite sign.

In Fig. 3c we have that the interaction between the flux density harmonic pairs of orders 34/36, 35/37, 104/106 and 105/107 contribute to increasing the total 2nd order radial force density. The interaction between the the harmonic pairs of orders 33/35, 103/105 and 106/108 contributes to a reduction in the total 2nd order radial force density.

Based on Fig. 3 it can be concluded that the 2nd order force component is mainly produced by the interaction between the main flux density harmonic and the two flux density components adjacent to the main harmonic. These harmonics have very small amplitudes in no-load operation. It can be seen from Table II that the 2nd order radial force component is very small in no-load. Based on this it can be concluded that the harmonics of the stator mmf produce most of the lowest order radial force component.

TABLE II:
2nd order radial force component at different loading

Generator:	F_2 (N/m^2)	
	No-load	Full-load
114-slot/14-pole	1253	27610
180-slot/14-pole	387	13140
432-slot/70-pole	521	5671

IV. EFFECTS OF WINDING LAYOUT

The flux density harmonic components adjacent to the main harmonic are the ones that produce most of the lowest order radial force component. In Table III the two adjacent harmonics to the main flux density harmonic are presented for no-load and full-load. The amplitude of the main harmonic is the same in both load conditions. One can see that for the 180-slot and the 114-slot generators, the harmonic of order $p+2$ is more or less independent of loading. In addition, this flux density harmonic is much smaller than the harmonic of order $p-2$.

The harmonic of order $p-2$ is mostly given by the armature mmf. Together with the main harmonic it is the main contributor to the lowest order radial force component. It is of interest to find a winding arrangement that minimize this flux density harmonic while maintaining the amplitude of the main harmonic.

For the 432-slot generator, Table III, one can see that harmonic of order $p-2$ is barely affected by loading. The

harmonic of order $p+2$ is the largest contributor to the lowest order force component together with the main harmonic. It is seen that this flux density harmonic component is present both at no-load and full-load.

TABLE III:
Flux density harmonics of order $p \pm 2$

Generator:	B_{p-2} (T)		B_{p+2} (T)	
	No-load	Full-load	No-load	Full-load
114-slot/14-pole	0.003	0.063	0.005	0.005
180-slot/14-pole	0.003	0.024	0.004	0.006
432-slot/70-pole	0.017	0.014	0.019	0.027

The 114-slot/14-pole generator is chosen in order to investigate how the winding layout pattern is affecting the flux density harmonic of order $p-2$. This generator has the largest 2nd order force component and the flux density component of order $p-2$. The winding pattern of the original winding is 3-3-3-2-3-3-2, see Table IV.

TABLE IV:
Winding layout

Original configuration						
RRR	-T-T-T	SSS	-R-R	TTT	-S-S-S	RR
-T-T-T	SSS	-R-R-R	TT	-S-S-S	RRR	-T-T
SSS	-R-R-R	TTT	-S-S	RRR	-T-T-T	SS
New configuration						
RRR	-T-T-T	SSS	-R-R	TT	-S-S-S	RRR
-T-T-T	SSS	-R-R-R	TT	-S-S	RRR	-T-T-T
SSS	-R-R-R	TTT	-S-S	RR	-T-T-T	SSS

Slots are marked with their assigned phase (R, S, T)

It is found that the pattern can be ordered in 21 possible configurations. All these patterns were implemented ans simulated. Of all the possible patterns, a pattern giving one of the lowest flux density component of order $p-2$ while barely reducing the main harmonic was selected. The new winding pattern is 3-3-3-2-2-3-3, see Table IV, and the comparison to the original winding pattern is shown in Table V. Several winding configurations gave a satisfying reduction in the flux density harmonic of order $p-2$, but they also gave a significant reduction in the main harmonic.

TABLE V:
Effects of changing the winding pattern

Layout:	B_1 (T)	B_{p-2} (T)	B_p (T)	B_{p+2} (T)	F_2 (N/m^2)
Original	0.075	0.063	1.038	0.005	27610
New	0.15	0.023	1.025	0.005	10860

One can see from Table V that the reduction in the flux density harmonic of order $p-2$ is 63.5 %. The 2nd order radial force component sees a 60.7 % reduction when the winding pattern is changed. The flux density harmonic of order $p+2$ remains unchanged while the main harmonic component sees a 1.25 % reduction.

Since both subharmonic components and harmonic components are produced by the winding pattern, it was expected that these could change with new winding patterns. It turned out that for all the patterns implemented and simulated, the

harmonic flux density components with harmonic order k times p remained practically unchanged ($k = 3, 5, 7$, etc).

The subharmonic flux density component of order 1 was found to change considerably with the change in winding pattern. As can be seen in Table V this component was doubled in in new pattern compared to the original winding layout. It seems that a reduction in the flux density harmonic of order $p - 2$ is giving an increase in the first order harmonic. The increase in the first order flux density harmonic increases the 2nd order force component. This helps explaining why the reduction in the lowest order radial force component is smaller than the reduction in the flux density harmonics of order $p - 2$ and p.

Two main conclusions may be drawn from this. First, that the amplitude of the largest flux density harmonic adjacent to the main harmonic can be heavily reduced by careful rearrangement of the winding configuration. Second, that in cases where low order radial forces cause vibration problems, the problem can be significantly reduced by rearranging the winding configuration. Again, this reinforces the conclusions made in [8] and [6] about the usefulness of winding-reconfiguration when the goal is to reduce low order radial forces.

V. CHANGING THE AIRGAP LENGTH

In [4] it was found that the cost of the generator is reduced when the synchronous reactance is increased by reducing the airgap length. In this section the influence on the lowest order radial force component of reducing the airgap length is investigated. The main flux density harmonic is kept constant when the airgap length is reduced.

The effect of reducing the airgap length on the radial force component of lowest harmonic order is presented in Table VI. One can see that reducing the airgap length to as little as 60 % of its initial value leads to modest increases in the radial force component. Reducing the airgap length to 60 % increases the lowest order force component of the 432-slot generator by 47.6 %, the 114-slot generator by 40.2 % and the 180-slot generator by 22.3 %. If one assume the increase in the 2nd order radial force component to be proportional to the reduction in airgap length, the increase should have been 66.7 %.

For the 14-pole generators, it is the flux density component of order $p - 2$ that interact with the main harmonic to produce most of the 2nd order radial force density. One can see from Table VI that the increase in this component closely resembles the increase in the 2nd order force component. For the 114-slot/14-generator the increase in the flux density component of order $p - 2$ was 36.5 % while the force component increased with 40.2 %. The same case can be seen for the 180-slot/14-pole generator where the flux density harmonic of order $p - 2$ increased 29.2 % while the force increased 22.3 %. The same effect is seen for the 432-slot/70-pole generator. The only difference is that for this generator it is the flux density harmonic of order $p + 2$ and not $p - 2$ in interaction with the main harmonic that produces most of the 2nd order radial force.

TABLE VI:
Effects of changing the airgap length

Slots/poles	114/14		180/14		432/70	
Airgap (mm)	35 o	22 r	27 o	16 r	25 o	15 r
B_{p-2} (T)	0.063	0.086	0.024	0.031	0.014	0.014
B_p (T)	1.04	1.06	1.14	1.17	1.017	1.016
B_{p+2} (T)	0.005	0.011	0.006	0.006	0.027	0.033
F_2 (N/m^2)	27610	38710	13140	16070	5671	8370

o - original and r - reduced airgap.

Table VII presents the distribution of magnetic energy in the different parts of the the generators at different airgap lengths. Values for the different parts are given in percent of the total magnetic energy, which is proportional to the magnetic reluctance. A high percentage means a high reluctance, which means that a large share of the magnetic energy is consumed in the given part.

TABLE VII:
Magnetic energy in different parts of the generators

Slots/poles	114/14		180/14		432/70	
Airgap (mm)	35 o	22 r	27 o	16 r	25 o	15 r
Airgap (%)	81.0	77.2	50.8	41.2	75.1	71.3
Stator yoke (%)	0.4	0.8	1.5	2.3	0.6	1.0
Stator teeth (%)	0.7	1.5	0.3	0.5	1.5	3.4
Pole core (%)	10.1	11.7	36.3	41.9	6.6	7.6
Rotor ring (%)	2.0	2.4	7.3	8.5	8.6	8.1
Total (kJ/m)	269	207	339	288	559	404

(%) of the total magnetic energy, o/r - original/reduced airgap.

One can see that the main part of the magnetic energy is stored in the airgap. For the 114-slot/14-pole and 432-slot/70-pole generators 71-81 % of the magnetic energy is consumed in the airgap. For the 180-slot/14-pole generator 40 to 51 % is consumed in the airgap.

In [6] it was assumed that all the magnetic energy was consumed in the airgap. This study has shown that this is not the case for large synchronous hydrogenerators. Using only the airgap permeance function and the stator mmf harmonics are not sufficient to calculate the amplitude of the airgap flux density harmonics correctly. With 20 to 50 % of the magnetic energy not being consumed in the airgap, it is clear that finite element simulations are needed.

Based on Table VI it is concluded that in salient pole synchronous hydrogenerators a reduction in the airgap length will not result in a linear increase in the lowest order radial force component as was predicted by [6].

VI. LOAD DEPENDENCY, SATURATION AND LOSSES

Load dependency on the 2nd order radial force component of the 180-slot/14-pole generator is explored in Fig. 4. Since the 2nd order force component is mainly produced by the interaction between the main flux density harmonic and the adjacent harmonics produced by the stator winding mmf, the amplitude of the force component increase with increasing load.

With linear material properties in the magnetic circuit of the generator, one would expect a proportional increase in the

radial forces with increasing loading of the stator windings. As can be seen in Fig. 4, this is clearly not the case. The main cause for the 2nd order component is the product of the flux density harmonics of order $p-2$ and p. It is seen that the change in the force component follows the same slope as flux density harmonic of order $p-2$. The main flux density harmonic remains more or less constant.

As the loading of the stator winding increases, the flux density component of order $3p$ increase. This leads to more saturation in the generator, which will reduce the increase of the flux density harmonic of order $p-2$. Increasing the loading beyond 100 % increases the saturation even more, which leads to a reduction in both the flux density harmonics adjacent to the main harmonic and the 2nd order radial force component.

When the distribution of magnetic energy in the generators are studied in Table VII it is seen that the share of the total energy consumed in the airgap is reduced when the airgap is reduced. This is because the saturation level increase in all the iron parts in the magnetic circuit. Except for the airgap, the pole core and rotor ring are the parts that has the highest share of magnetic energy. Especially the pole core which has to conduct all the flux produced by the field winding are likely to be saturated.

The 180-slot/14-pole generator has a significantly higher saturation level in the pole core and share of the magnetic energy than the other generators. A consequence of this is that the amplitude of the flux density harmonics in the airgap of the 180-slot/14-pole generator is smaller than would have been the case with a less saturated pole core.

A more saturated generator seems to reduce the lowest order spatial harmonic of the radial force density distribution through a reduction in the amplitude of the flux density harmonics adjacent to the main flux density harmonic. The downside to increasing the saturation is increased losses in the iron parts. Increased saturation seems to happen when the airgap length is reduced.

Losses in the pole shoe surface, and in the damper bars if damper bars are installed, are expected to increase when the airgap length is reduced. The analytical framework used in [4] are used to estimate the pole surface and damper bar losses in this case. In the the 180-slot/14-pole generator the losses increased from 4.8 kW to 12.4 kW, while the losses increased from 18.0 kW to 42.4 kW in the 432-slot/70-pole generator. For the 114-slot/14-pole generator, the losses increased from 35.9 kW to 89.1 kW.

The damper bars are not included in this paper, as they are expected to reduce the amplitudes of the harmonics in the airgap flux density. A full analysis of the effect of damper bars on the lowest order radial force component are left out for a future work. This will require a full, time-stepping finite element simulation where both the impact on the radial forces and the losses in the damper bars should be considered.

VII. Conclusions

It has been found that the lowest order harmonic component of the radial force is produced primarily by the main
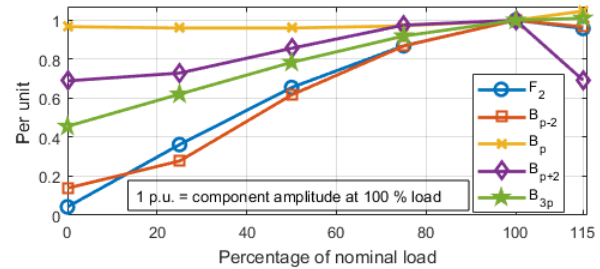

Fig. 4: Effect of loading on the 2nd order radial force component in the 180-slot/14-pole generator.

flux density harmonic component and its adjacent harmonic components. In salient pole synchronous hydrogenerators, the magnetic circuit can be heavily loaded. In the cases investigated here, more than 20 % of the magnetic energy is consumed in other parts of the generator than the airgap. Reducing the airgap length leads to a less than proportional increase in the lowest order radial force component due to increased saturation in the generator and the fact that a substantial part of the magnetic energy is not consumed in the airgap. A rearrangement of the winding layout is found to be an effective method for reducing the lowest order radial force component. In order to calculate the flux density harmonics and the radial forces in large synchronous hydrogenerators accurately, it is found that finite element simulations are needed.

References

[1] J. Pyrhönen, T. Jokinen, and V. Hrabovcová, *Design of Rotating Electrical Machines*, 2nd ed. John Wiley & Sons, Ltd, 2014.

[2] G. Traxler-Samek, T. Lugand, and M. Uemori, "Vibrational Forces in Salient Pole Synchronous Machines Considering Tooth Ripple Effects," *IEEE Transactions on Industrial Electronics*, vol. 59, no. 5, pp. 2258–2266, 2012.

[3] M. Valavi and A. Nysveen, "Variable-Speed Operation of Hydropower Plants: Past, Present and Future," in *2016 XXII International Conference on Electrical Machines (ICEM)*, 2016, pp. 640–646.

[4] E. L. Engevik, T. E. Hestengen, M. Valavi, and A. Nysveen, "Effects of lifting reactance requirements on the optimal design of converter-fed synchronous hydrogenerators," in *2017 IEEE International Electric Machines and Drives Conference (IEMDC)*, 2017.

[5] M. Valavi, A. Nysveen, R. Nilssen, R. D. Lorenz, and T. Rølvåg, "Influence of pole and slot combinations on magnetic forces and vibration in low-speed PM wind generators," *IEEE Transactions on Magnetics*, vol. 50, no. 5, pp. 1–11, 2014.

[6] T. Lugand and A. Schwery, "Comparison between the salient-pole synchronous machine and the double-fed induction machine with regards to electromagnetic parasitic forces and stator vibrations," in *2016 XXII International Conference on Electrical Machines (ICEM)*, 2016, pp. 2191–2197.

[7] T. Lugand, "Contribution to the Modeling and Optimization of the Double-Fed Induction Machine for Pumped-Storage Hydro Power Plant Applications," Ph.D. dissertation, Université de Grenoble, 2013.

[8] B. Taraldsen, "Statorschwingungen in synchronmaschinen mit bruchlochwicklungen (In German)," *Dr. Ing. dissertation, Norwegian Institute of Technology (NTH)*, 1985.

[9] M. M. Liwschitz, "Distribution Factors and Pitch Factors of the Harmonics of a Fractional-Slot Winding," *Transactions of the American Institute of Electrical Engineers*, vol. 62, no. 10, pp. 664–666, 1943.

[10] M. Valavi, J. Pascal, and A. Nysveen, "Analysis of radial magnetic forces in hydrogenerators with fractional-slot windings," in *2016 XXII International Conference on Electrical Machines (ICEM)*, 2016, pp. 1318–1324.